Computational Materials Science 49 (2010) S60–S64

Contents lists available at ScienceDirect

Computational Materials Science

journal homepage: www.elsevier.com/locate/commatsci

Modeling and simulation of buckling of polymeric membrane thin film gel

Zishun Liu [a,*], Wei Hong [b], Zhigang Suo [c,**], Somsak Swaddiwudhipong [d], Yongwei Zhang [a]

[a] Institute of High Performance Computing, Singapore 138632, Singapore
[b] Dept. of Aerospace Engineering, Iowa State University, Ames, IA 50014, USA
[c] School of Engineering and Applied Sciences, Harvard University, Cambridge, MA 02138, USA
[d] Dept. of Civil Engineering, National University of Singapore, Singapore 119260, Singapore

ARTICLE INFO

Article history:
Received 29 August 2009
Received in revised form 25 November 2009
Accepted 11 December 2009
Available online 29 April 2010

Keywords:
Gel
Swelling
Deswelling
Finite element method
Buckling

ABSTRACT

The swelling- and deswelling-induced instabilities of various membrane structures are simulated using the inhomogeneous field theory of a polymeric network in equilibrium with a solvent and mechanical load/constraint and the Finite Element subroutine developed in ABAQUS. The simulating results of these membrane gels are compared with available experimental results, and a reliable prediction in deformation pattern and critical conditions has been achieved. The study has been made in attempt to mimic the shape of a plant leaves from the swelling/deswelling patterns of a gel. Furthermore, this study provides a possibility to explore the origin of intriguing natural phenomena of plants.

1. Introduction

Polymeric gels have recently attracted more attention, due to their unparalleled responsiveness to stimuli of various kinds, such as temperature, pH value, ionic strength and humidity [1–7]. For example, a volumetric swelling ratio up to 1000% has been reported in the literature [8,9]. In addition to its capability of significant shape and volume changes in response to stimuli, its biocompatibility and softness assure a promising future in the area of bioengineering and drug delivery [10–13]. Indeed, many natural tissues of plants and animals are to some extent polymeric gels [13]. Mixtures of macromolecular networks and solvents also constitute most tissues of plants and animals, where the networks retain the general shape and the solvents enable the transport of nutrients and wastes. This implies that the growth of some plants is analogous to the swelling of polymeric gel. The natural growth processes in some leaves and flowers could lead to a complex three-dimensional fractal shapes while some living organisms are full of fascinating complex patterns and shapes in the natural growth [14–16]. One might wonder about how a simple deformation process, e.g. the opening and closure of flowers [16] leads to such complex shapes, and what the underlying physical mechanisms are. How to explain the mechanism of flower deformations in flower opening and closure? How to elucidate the morphogenesis and the natural growth of some leaves, flowers and vesicles? According to our study, the inhomogeneous gel deformation theory may be used to clarify this phenomenon.

Gels in the form of a thin sheet are commonly present in both synthetic and natural structures. The thin polymeric gel film can develop a variety of off-plane deformation patterns during swelling or deswelling, when part of it is constrained [17–25]. Similarly, flower petals and leaves, for example, also can develop diverse three-dimensional structures during growth. Some of the growth patterns may be attributed to the consequence of gel swelling/deswelling [15,16].

Due to constraints, neither the solvent concentration nor the stress field in the gel film is homogeneous even in equilibrium [24,26,27]. Therefore, applying a free-swelling result directly to a constrained deformation of gel film will lead to erroneous results. In this paper, we try to verify the inhomogeneous field theory of a polymeric gel in equilibrium and the subroutine implemented into ABAQUS [27]. Furthermore we propose a new application area for gel large deformation, i.e. plant deformation. We investigate the buckling patterns induced by the constrained swelling or deswelling of polymeric gel film, using our recently developed finite-element code [27]. We will look at the constrained swelling process of rectangular and circular gel films. The buckling patterns of such gel films are simulated and compared with available test results in the literature. For circular annulus gel film, the buckling patterns may be used to explain the shapes of the flowers. As another

* Corresponding author. Address: Institute of High Performance Computing, 1 Fusionopolis Way, #16-16 Connexis, Singapore 138632, Singapore. Tel.: +65 6419 1289; fax: +65 6419 1280.
** Corresponding author.
E-mail addresses: liuzs@ihpc.a-star.edu.sg (Z. Liu), suo@seas.harvard.edu (Z. Suo).

0927-0256/$ - see front matter © 2010 Elsevier B.V. All rights reserved.
doi:10.1016/j.commatsci.2009.12.036

example, we also investigate the swelling pattern of a gel film in the shape of a plant leaf, trying to mimic the work of Mother Nature.

2. Gel inhomogeneous field theory and implementation of numerical simulation

Consider a network of polymers in contact with a solvent, subject to a mechanical load and geometric constraint, and held at a constant temperature. If we take the stress-free dry network as the reference state, the deformation gradient of the network is defined as [24]:

$$F_{iK} = \frac{\partial x_i(\mathbf{X})}{\partial X_K}. \tag{1}$$

where X_i and $x_i(\mathbf{X})$ are the network coordinates of gel system at reference and deformed states, respectively. In the deformed state, introduce $C(\mathbf{X})dV(\mathbf{X})$ as the number of solvent molecules in the element of volume $dV(\mathbf{X})$. Thus, the combination of the two fields $x_i(\mathbf{X})$ and $C(\mathbf{X})$ can describe the state of the gel system in which the field $x_i(\mathbf{X})$ describes the deformation of the network, while the field $C(\mathbf{X})$ describes the distribution of the solvent molecules in the gel system.

Let $WdV(\mathbf{X})$ be the Helmholtz free energy of the gel in the element of volume $dV(\mathbf{X})$ and the gel be in a state of equilibrium characterized by the two fields, $x_i(\mathbf{X})$ and $C(\mathbf{X})$. We assume that the free-energy density of the gel, W, is a function of the deformation gradient of the network, $\mathbf{F}$, and the concentration of the solvent in the gel, C. When the gel equilibrates with the solvent and the mechanical load, the chemical potential (μ) of the solvent molecules is homogeneous in the external solvent and in the gel:

$$\mu = \frac{\partial W(\mathbf{F}, C)}{\partial C}. \tag{2}$$

Thermodynamics dictates that the change in the free energy of the gel should equal the sum of the work done by the external mechanical force and by the external solvent, namely,

$$\int \delta W dV = \int B_i \delta x_i dV + \int T_i \delta x_i dA + \mu \int \delta C dV. \tag{3}$$

The first and second terms on right hand side of Eq. (3) represent mechanical work done by body force $B_i(\mathbf{X})dV(\mathbf{X})$ and surface force $T_i(\mathbf{X})dA(\mathbf{X})$, respectively. The third term is the work done by the external solvent. This equation holds for any small changes $\delta\mathbf{x}$ and δC from the state of equilibrium.

Introduce another free-energy function $\hat{W}$ by using a Legendre transformation:

$$\hat{W} = W - \mu C. \tag{4}$$

$\hat{W}$ is a function of the deformation gradient of the network and the chemical potential of the solvent molecules, i.e. $\hat{W}(\mathbf{F}, \mu)$.

A combination of Eqs. (3) and (4) gives that

$$\int \delta \hat{W} dV = \int B_i \delta x_i dV + \int T_i \delta x_i dA. \tag{5}$$

It should be noted that when the gel is in a state of equilibrium, the chemical potential of the solvent molecules inside the gel is homogeneous and is equal to the chemical potential of the external solvent, μ. Indeed, the chemical potential plays a role analogous to that of the temperature. The equilibrium condition (5) takes the same form as that for a solid mechanics. Once the function $\hat{W}(\mathbf{F}, \mu)$ is prescribed, we can implement a finite element method to solve it.

All molecules in a gel are taken to be incompressible, so that the volume of the gel is the sum of the volume of the dry network and the volume of the pure liquid solvent. We denote v as the volume per solvent molecule. Consequently, the concentration of the solvent in the gel relates to the deformation gradient of the network as [24]:

$$1 + vC = \det \mathbf{F}. \tag{6}$$

According to the well known Flory and Rehner theory [28] and Eq. (6), the modified free-energy function for polymeric gel can be expressed as [24]:

$$\hat{W}(\mathbf{F}, \mu) = \frac{1}{2} NkT(I - 3 - 2\log J) - \frac{kT}{v}\left[(J-1)\log\frac{J}{J-1} + \frac{\chi}{J}\right] - \frac{\mu}{v}(J-1), \tag{7}$$

where $I = F_{iK}F_{iK}$ and $J = \det \mathbf{F}$ are invariants of the deformation gradient, N is the number of polymeric chains per reference volume, kT is the absolute temperature in the unit of energy, and χ is a dimensionless measure of the enthalpy of mixing. When $\chi > 0$, the solvent molecules like themselves better than they like the long-chained polymers. In this free-energy function of gel, the deformation gradient of the network, $\mathbf{F}$, and the chemical potential of the solvent, μ, are the independent variables. The above theory was implemented in the finite element package, ABAQUS, by coding Eq. (7) into a user-defined subroutine for a hyperelastic material (UHYPER) or UMAT [27].

The nominal stress as the work conjugates to the deformation gradient can be defined as:

$$s_{iK} = \frac{\partial \hat{W}(\mathbf{F}, \mu)}{\partial F_{iK}}, \tag{8}$$

Inserting Eqs. (7) into (8), we can obtain the equation of state of the gel:

$$\frac{s_{iK}}{kT/v} = Nv(F_{iK} - H_{iK}) + \left[J\log\left(1 - \frac{1}{J}\right) + 1 + \frac{\chi}{J} - \frac{\mu}{kT}J\right]H_{iK}. \tag{9}$$

A representative value of the volume per molecule is $v = 10^{-28}\mathrm{m}^3$. At room temperature, $kT = 4 \times 10^{-21}$ J and $kT/v = 4 \times 10^7$ Pa. We take the following dimensionless parameters for the gel material that we used in simulations: $Nv = 0.001$, $\chi = 0.1$. In this study, these representative values are taken for all cases.

It should be noted that in the implementation of the inhomogeneous field theory of a polymeric gel, the free energy (7) is singular when the network is solvent-free, $vC = 0$. To avoid this singularity, we choose a reference state such that the network, under no mechanical load, equilibrates with a solvent of chemical potential μ_0, $vC > 0$. Relative to the dry network, the network in this state swells with isotropic stretches. We denote this free-swelling stretch by α_0, which relates to the chemical potential μ_0 by setting stress (9) to be zero.

3. Swollen thin films constrained on edges

As a first example, we study the deformation patterns of gel films while swollen. The films are constrained on one or two of their edges. Similar experimental studies have been carried out by Mora and Boudaoud [29]. In their experiments, they assembled the gel film from two parts which have distinct elastic and swelling properties. After reaching equilibrium with the solvent, the softer part of the film swells significantly while the stiffer one deforms negligibly. Since the stiffer gel hardly swells and the modulus is orders of magnitude higher than that of the softer gel, we replace them with rigid wall constraint in our simulations for computational efficiency. Gel films with two different geometries are studied herein: (i) a rectangular strip gel constrained on one or two side edges, and (ii) a circular annulus gel constrained on the inner edge.

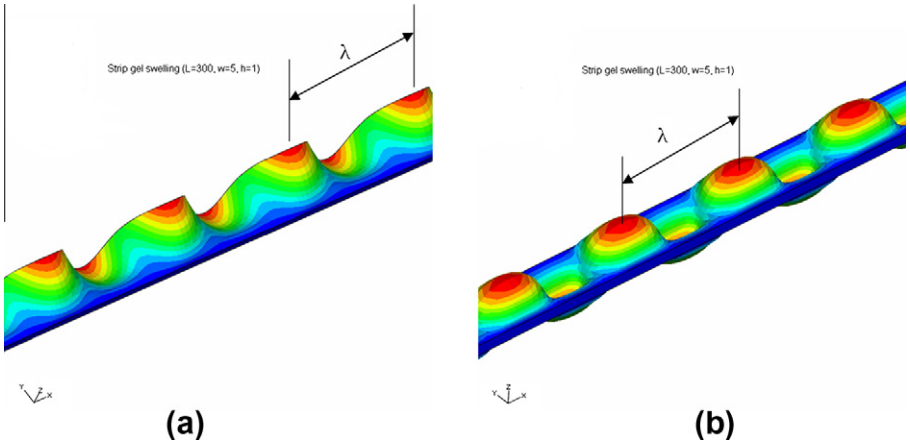

Fig. 1. The deformation pattern of rectangular strip membrane gel: (a) constrained along one edge; (b) constrained along two edges.

In the FEM modeling, 8-nodes brick element (C3D8) is used to model the strip thin film gel and circular annulus gel. The total numbers of elements are from 1200 to 4200 for strip structures with different width. While the total numbers of elements for corona geometry plates with different inner diameter are from 2500 to 7500.

3.1. A stripe gel constrained along one and two side edges

In this case, we study a rectangular gel strip, measures $L \times w \times H$, in length, width and thickness, respectively. Gel films of various widths, constrained at one or both side edges are investigated. The length of the strips are taken to be long enough, $L > 50w$, to minimize the end effect. The initial stretch of the gel swelling is taken to be $\alpha_0 = 2.5$, corresponding to a dimensionless chemical potential of $\mu/kT = -0.0013942$. It is assumed that the films are very thin so that the solvent molecules have enough time to migrate in them and reach equilibrium.

We first look at a gel strip constrained on one side edge. In the first stage of swelling, the film deforms almost uniformly, and it increases in thickness and width. The film is almost stress-free in the thickness direction and the width direction. However, in the longitudinal direction a large compressive stress is built up, due to the constraint at the two ends of the strip. When the swelling reaches a critical chemical potential value, the uniform deformation becomes unstable and the gel strip buckles into a three-dimensional deformation pattern, as shown in Fig. 1a. It is noted that the buckling pattern is periodic along the length of the strip, having almost a constant wavelength of λ, which is the same as the phenomenon observed experimentally by Mora and Boudaoud [29]. The deformation mechanism of this gel film can be explained as follows: for thin film structure, the bending rigidity of gel film is much smaller than their stretching rigidity. When gel swells, the compressive stress is generated along the longitude direction. To minimize the system elastic energy, the sheet buckles into the shapes that remove the in-plan compression [30].

The deformed pattern for gel strip constrained along two side edges is shown in Fig. 1b. The buckling model is similar to the first mode of strip structure under the same constraint. Along the length of the strip, the periodic deformed pattern is also observed, but the wavelength of gel strip with two side edges constraint is smaller than that of a single side edge constraint. For this case, the compressive stresses generated in the gel films are 2-dimensional. This is also consistent with the observation that the larger the compression, the smaller the possible wavelength of the buckles in crumpling of paper sheet.

In order to study the effect of the strip gel width on buckling model and deformation pattern, a series of the width values over the thickness of gel film are simulated for both types of constraint strip gels. We increase the ratio of width to thickness of strip gel film from $w/H = 1$–15. Fig. 2 shows the instability wavelength λ as a function of the width w of the swollen strips for both types of constraints. The wavelength and the width are normalized by the strip initial thickness, i.e. λ/H and w/H. It can be seen that the wavelength increases with the width w. The simulated results show the same trend as observed by Mora and Boudaoud in their experiment. Fig. 2 demonstrates that the wavelengths are higher than those of the analytical results of Foppl-von Karman linear stability theory for strip gel constrained along one side edge, but those of two side edges constraint are lower than the analytical values. If the aspect ratio of width to thickness w/H, is reduced to certain critical value, the strip becomes stable and the buckling is suppressed through out the swelling. The critical values of w/H are about 1.6 and 2.7 for one edge constrained strip and two-edge constrained strip gel respectively.

3.2. An annulus constrained along the inner edge

The next example involves the study on corona geometry gel swelling. The inner edges of the annulus gel are clamped. Similar

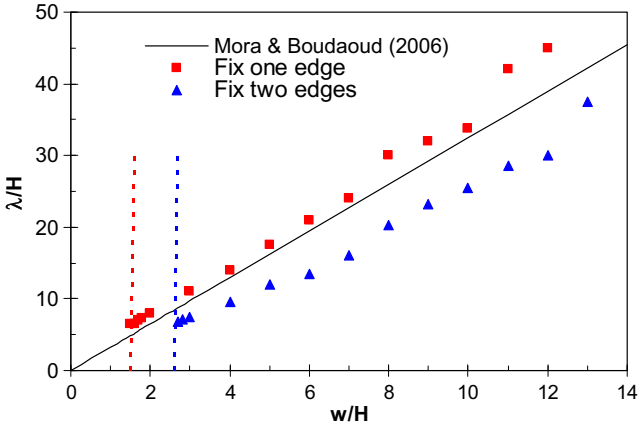

Fig. 2. The instability wavelength λ as a function of the width w of the swollen rectangular membrane strip gels for constraining one edge and two edges (the length of the strip is assumed very long, in present study $L/w > 50$), two dot lines represent the critical points of buckling commencing for one edge fixed and two edges fixed).

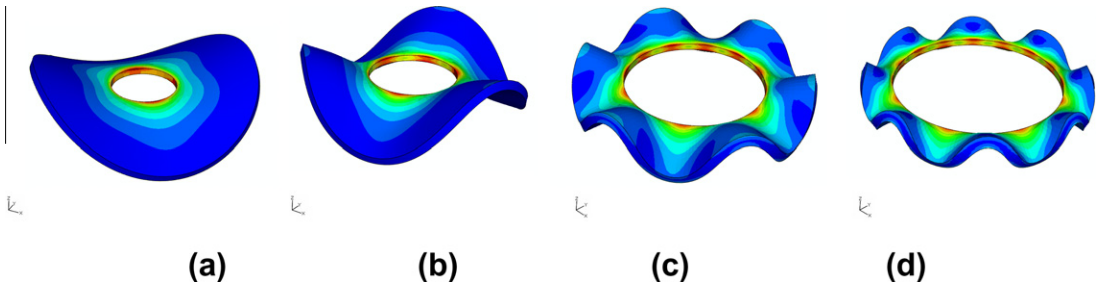

Fig. 3. The buckling shapes and the von-Mises stress distribution of corona membrane gels for different inner radius (the ratio of outer radius and thickness $R_0/H = 15$, initial chemical potential $\mu_0/kT = -0.001394203$, $\alpha_0 = 2.5$) (a) $R_i/H = 5$ (b) $R_i/H = 7$ (c) $R_i/H = 10$ (d) $R_i/H = 12$.

problems were studied earlier through experimental method by Mora and Boudaoud [29]. In their study, a disk of stiffer gel is clamped to a corona of softer swelling gel. No-swelling is assumed for hard gel but soft gel can. Mora and Boudaoud [29] observed that when the assembly of gel plate is swelling, the flat gel plate deforms and finally reaches the unstable buckling state. In the present study, the inner edge of annulus gel is assumed to be very stiff and hence no swelling deformation. In this simulation, the ratio of outer radius of annulus film gel and initial thickness R_0/H is kept constant at 15, while four different values of the ratio of inner radius of annulus gel film to thickness R_i/H, are 5, 7, 10 and 12 in the present study.

The final deformed patterns of gel swelling, are illustrated in Fig. 3a–d. As expected, it is observed that the larger number of buckling wave is associated with the increase in the inner radius of the annulus. The results are consistent with Mora and Boudaoud's experimental observation [29]. When the inner radius is small or the ratio of R_o/R_i becomes large, the final deformed pattern is the same as that noted for a circular plate where hyperbolic paraboloid or saddle shape is normally generated. When R_o/R_i approaches 1.2–1.5, the deformation pattern is similar to a strip gel film. The von-Mises stress distribution is also included in each case as depicted in Fig. 3. The maximum von-Mises stresses concentrate on the inner edge of annulus gel films. This is again in good agreement with Mora and Boudaoud's experimental observation [29]; they noted that whenever the structure is accidentally broken, the failure always occurs in connection of the bulk of the soft part.

The deformation patterns of these corona gel films can be used to explain some flower/leave patterns. In nature, the wavy patterns or shapes can be observed along the outer edges of the cabbage flower leaves. During the growth of the plant leaves, the inner part of the circular leaves is normally stiffer than that of the outer surface area and the tissue growth along the leaf outer edges induces the wrinkling and wavy patterns of the leaf edge. From mechanics point of view, the phenomenon arises from the energy minimization of plant under growing. This wrinkling allows relaxation of the resulting strain in the leaf growth.

4. Leaf swelling and deswelling

Natural growth and living organisms are full of fascinating complex patterns and shapes. One might wonder about the physical mechanisms of these structural deformations, such as those of leaves and flowers. These natural phenomena have long drawn attention from botanical scientists. However, the topic of how to explain the morphogenesis and the natural growth of leaves is still not yet readily available. In leave growth, a flower leave can present a three-dimensional out-of-plane deformed pattern. Since many plant tissues can be regarded as polymeric gel to certain extent, the buckling patterns of gel membrane under swelling and deswelling may be used to explain this interesting deformation pattern. Strictly speaking, the gel is different from the living tissues of plant, but the mechanism of leave growth is similar to the gel swelling/deswelling phenomena. The growing process of a plant leaf is similar to the gel swelling; whereas the drying or senescence process of a leaf is analogous to the membrane gel deswelling [15,16]. In this example, we present an analogy of plant leaves growing and drying processes by observing swelling and deswelling of gel materials, respectively.

The elliptical membrane gel with the ratio of major axis to thickness, $a/H = 150$, and the ratio of minor axis to thickness, $b/H = 50$ is modeled for a leaf initial shape. The leaf surface is modeled by polymer gel material which has certain initial deformation in two-dimensional plane. The leaf stem is modeled as a stiffener frame with stiffer elastic materials along the major axis. In the modeling, one end of the ellipse major axis is fixed. To simplify the problem, the initial configurations of the leaf are assumed to be flat. In the FEM modeling, the leaf surface is model by 8-node brick element (C3D8) and stem is modeled by beam element (B21). A few thousand elements are used for leaf structure. In the simulation, we vary the chemical potential of the gel and to mimic the leaf drying process, the gel is assumed to be deswelling and the chemical potential of the gel decreases gradually. The chemical potentials of the gel leaf vary from a base value of zero for the initial state reaching the final value of $\mu/kT = -6.36 \times 10^{-5}$ in this simulation. The initial and final deswelling patterns of gel leaf are illustrated in Fig. 4a and b. It can be seen that the buckling of gel leaf membrane takes place in the deswelling process and the flat surface deforms to a three-dimensional pattern. During the closing of the leaf from the flat surface to the curved surface, the stiffer stem of the leaf is also bent to minimize the free energy of the system. The simulated deformation pattern of the leaf as shown in Fig. 4b is similar to that of some natural leaf senescence.

To simulate the leaf grown process, we increase the gel chemical potential from an initial value of $\mu_0/kT = -0.00139420$ to the final value of $\mu/kT = -0.001279$. The initial and final deformation patterns of gel leaf swelling are shown in Fig. 4c and d respectively. It can be observed that the flat membrane of the leaf gel deforms into a hyperbolic parabolic (saddle) shape. This demonstrates that the gel leaf membrane is buckling when swelling. Though artificial values are assumed for the material properties of leaf gel membrane and the example does not give the actual values of deformation and the deformed shape of a gel leaf growing or drying processes exactly, the study provides a useful methodology for further studying of actual leaf growing and senescence. The example explains the physical mechanism of plant leaf growing and drying, and the fascinating complex deformation patterns of the leaf and flower via simulation through gel swelling and deswelling processes. Once the values of the natural leaf material properties are available, the detailed deformation pattern of the leaf can be quan-

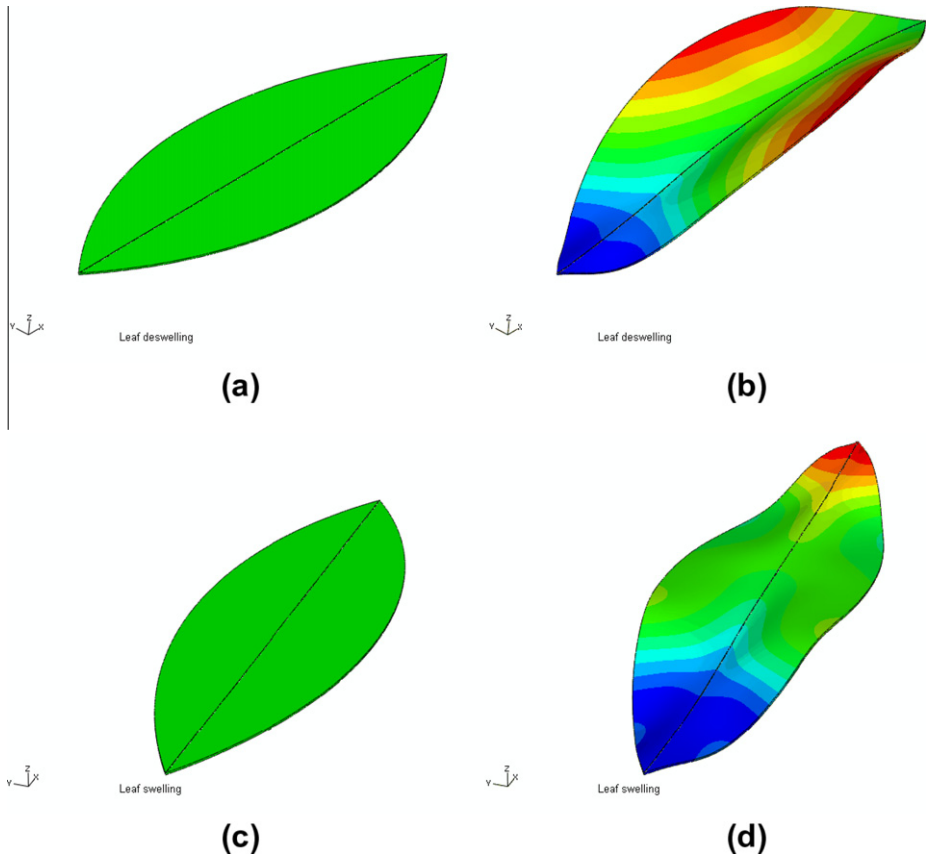

Fig. 4. The deformation patterns of a leaf at drying/growing by using membrane gel deswelling/swelling, (a) the initial configuration of gel leaf for drying, (b) the deformed pattern of gel leaf at certain drying stage (c) the initial configuration of gel leaf when growing, (d) the deformation pattern of gel leaf when it swells to certain stage. (For interpretation of the references to colour in this figure legend, the reader is referred to the web version of this article.)

titatively predicted and simulated based on the same procedure adopted herein. The methodology and simulation process also provide the great potential for further study on flowers and leaves evolutions under various environmental conditions.

5. Concluding remarks

In this study, the inhomogeneous field theory of polymeric network in equilibrium with solvent and mechanical load or constraint is further investigated through modeling and simulation of polymeric thin film membrane gels. This paper studied the swelling-induced and deswelling-induced instabilities of membrane gel structures based on the inhomogeneous field theory which has been implemented in the finite element package, ABAQUS. The buckling phenomena of membrane gels are simulated and the results are compared with available experimental results. It was demonstrated that using present field theory and the developed user subroutine of finite element method, the membrane gel deformation pattern in buckling cases can be simulated and predicted. The paper also first reports examples demonstrating the possibility of studying the natural plant tissue deformation in growing or senescence processes via the application of membrane gel swelling or deswelling and hence the fantasying phenomena of nature may be scientifically explained. We hope that this field theory and the developed FE subroutine will motivate more future research to elucidate more complex natural phenomena. The study may also be extended to assist the design of physical growing tissues by varying the gel parameters. It is also possible for us to control the flower opening pattern by changing the stimuli environment.

References

[1] Z.B. Hu, X.M. Zhang, Y. Li, Science 269 (1995) 525.
[2] F. Horkay, G.B. McKenna, Polymer networks and gels, in: J.E. Mark (Ed.), Physical Properties of Polymers Handbook, Springer, New York, 2007, p. 497.
[3] A. Sidorenko, T. Krupenkin, A. Taylor, P. Fratzl, J. Aizenberg, Science 315 (2007) 487.
[4] D.J. Beebe, J.S. Moore, J.M. Bauer, Q. Yu, R.H. Liu, C. Devadoss, B.H. Jo, Nature 404 (2000) 588.
[5] J. Dolbow, E. Fried, H. Ji, Comput. Methods Appl. Mech. Eng. 194 (2005) 4447.
[6] H. Li, R. Luo, E. Birgersson, K.Y. Lam, J. Appl. Phys. 101 (2007) 114905.
[7] K.K. Westbrook, H.J. Qi, J. Intell. Mater. Syst. Struct. (2007), doi:10.1177/1045389X07077856.
[8] Y. Hirose, T. Amiya, Y. Hirokawa, T. Tanaka, Macromolecules 20 (1987) 1342.
[9] G.D. Nicodemus, S.J. Bryant, J. Biomech. 41 (2008) 1528.
[10] O. Wichterle, D. Lim, Nature 185 (1960) 117.
[11] N.A. Peppas, J.Z. Hilt, A. Khademhosseini, R. Langer, Adv. Mater. 18 (2006) 1345.
[12] L. Dong, A.K. Agarwal, D.J. Beebe, H.R. Jiang, Nature 442 (2006) 551–554.
[13] M. Rinaudo, Polym. Int. 57 (2008) 397.
[14] E. Sharon, B. Roman, M. Marder, G.S. Shin, H.L. Swinney, Nature 419 (2002) 579.
[15] T.E. Gookin, D.A. Hunter, M.S. Reid, Plant Sci. 164 (2003) 769.
[16] W.G. van Doorn, U. Meeteren, J. Exp. Bot. 54 (2003) 1801.
[17] Y. Klein, E. Efrati, E. Sharon, Science 315 (2007) 1116.
[18] S. Ladet, L. David, A. Domard, Nature 452 (2008) 76.
[19] C.J. Durning, K.N. Morman, J. Chem. Phys. 98 (1993) 4275.
[20] E. Cerda, L. Mahadevan, Phys. Rev. Lett. 90 (2003) 074302.
[21] Y. Zhang, E.A. Matsumoto, A. Peter, P.C. Lin, R.D. Kamien, S. Yang, Nano Lett. 8 (2008) 1192.
[22] V. Trujillo, J. Kim, R.C. Hayward, Soft Matter 4 (2008) 564.
[23] B.W. Francoise, G. de Pierre, Science 300 (2003) 441.
[24] W. Hong, X.H. Zhao, J.X. Zhou, Z.G. Suo, J. Mech. Phys. Solids 56 (2008) 1779.
[25] T. Mullin, S. Deschanel, K. Bertoldi, M.C. Boyce, Phys. Rev. Lett. 99 (2007) 084301.
[26] X.H. Zhao, W. Hong, Z.G. Suo, Appl. Phys. Lett. 92 (2008) 051904.
[27] W. Hong, Z.S. Liu, Z.G. Suo, Int. J. Solids Struct. 46 (2009) 3282.
[28] P.J. Flory, J. Rehner, J. Chem. Phys. 11 (1943) 521.
[29] T. Mora, A. Boudaoud, Eur. Phys. J. E 20 (2006) 119–124.
[30] T. Mora, A. Boudaoud, Phys. Rev. Lett. 91 (2003) 680105.